Biochemical and Biophysical Research Communications 440 (2013) 56–61

Contents lists available at ScienceDirect

Biochemical and Biophysical Research Communications

journal homepage: www.elsevier.com/locate/ybbrc

The effect of exposing a critical hydrophobic patch on amyloidogenicity and fibril structure of insulin

Yang Li [a], Lianqi Huang [a], Xin Yang [a], Chen Wang [a], Yue Sun [b], Hao Gong [a], Yang Liu [a], Ling Zheng [b], Kun Huang [a,c,*]

[a] Tongji School of Pharmacy, Huazhong University of Science & Technology, Wuhan, Hubei 430030, PR China
[b] College of Life Sciences, Wuhan University, Wuhan, Hubei 430072, PR China
[c] Centre for Biomedicine Research, Wuhan Institute of Biotechnology, Wuhan, Hubei 430075, PR China

ARTICLE INFO

Article history:
Received 29 August 2013
Available online 13 September 2013

Keywords:
Porcine insulin
Desoctapeptide-(B23–B30) insulin (DOI)
Amyloidogenicity
Fibril structure
Membrane damage
Hemolysis

ABSTRACT

It is widely accepted that the formation of amyloid fibrils is one of the natural properties of proteins. The amyloid formation process is associated with a variety of factors, among which the hydrophobic residues play a critical role. In this study, insulin was used as a model to investigate the effect of exposing a critical hydrophobic patch on amyloidogenicity and fibril structure of insulin. Porcine insulin was digested with trypsin to obtain desoctapeptide-(B23–B30) insulin (DOI), whose hydrophilic C-terminal of B-chain was removed and hydrophobic core was exposed. The results showed that DOI, of which the ordered structure (predominantly α-helix) was markedly decreased, was more prone to aggregate than intact insulin. As to the secondary structure of amyloid fibrils, DOI fibrils were similar to insulin fibrils formed under acidic condition, whereas under neutral condition, insulin formed less polymerized aggregates by showing decreased β-sheet contents in fibrils. Further investigation on membrane damage and hemolysis showed that DOI fibrils induced significantly less membrane damage and less hemolysis of erythrocytes compared with those of insulin fibrils. In conclusion, exposing the hydrophobic core of insulin can induce the increase of amyloidogenicity and formation of higher-order polymerized fibrils, which is less toxic to membranes.

1. Introduction

The deposition of proteins has been found to be associated with over twenty diseases, such as Alzheimer's and Prion diseases [1,2]. To discover pathological mechanism and new therapeutic approaches of these diseases, a lot of work has been done to understand the progress of amyloid fibril formation and many intrinsic factors have been found to be related to amyloid fibril formation, including amino acid sequence, disulfide bond and so on [3,4]. Among these factors, the hydrophobic residues play an important role [5,6]. In aqueous solution, minimizing the number of hydrophobic side chains exposed to water is the principal driving force for hydrophobic interaction [7], which drives hydorphobic residues interacting with each other and leads to the formation of oligomers, protofibrils and amyloid fibrils [8]. On the other hand, the process of amyloid fibril formation can be inhibited by masking the hydrophobic residues [9].

Here, we chose insulin as a model to investigate the effect of exposing a critical hydrophobic patch on amyloid fibril formation of insulin. The native structure of insulin under physiological condition is mainly helical, with two chains linked by two inter-chain disulfide bonds. We have previously demonstrated that certain hydrophobic residues residing the hydrophobic core, like Val^{A3} and Val^{B12}, are essential for receptor binding and activity [10,11]. During amyloid formation, the initial step is related to the displacement of the B-chain C-terminal region that exposes the hydrophobic core [12]. Our previous study also showed that foreshortening the connecting peptide of proinsulin markedly retards the fibrillation [13], possibly by stabling conformation and avoiding exposure of hydrophobic residues [14].

However, the effect of exposing the critical hydrophobic core on amyloid formation remained unclear. In this study, a critical hydrophobic patch exposed insulin analog, desoctapeptide-(B23–30) insulin (DOI, Fig. 1A and B), was obtained by removing the C-terminal of B-chain; and this analog was used to investigate the effect of exposing the hydrophobic patch on amyloid formation

Abbreviations: DOI, desoctapeptide-(B23–B30) insulin; RP-HPLC, reversed phase high performance liquid chromatography; CD, circular dichroism; ThT, thioflavin-T; TEM, transmission electron-microscopy; POPG, 2-oleoyl-1-palmitoyl-sn-glycerol-3-phospho-rac(1-glycerol) sodium salt; POPC, 2-oleoyl-1-palmitoyl-sn-glycero-3-phosphocholine.

* Corresponding author at: Tongji School of Pharmacy, Huazhong University of Science & Technology, Wuhan, Hubei 430030, PR China.
E-mail address: kunhuang2008@hotmail.com (K. Huang).

0006-291X/$ - see front matter © 2013 Elsevier Inc. All rights reserved.
http://dx.doi.org/10.1016/j.bbrc.2013.09.032

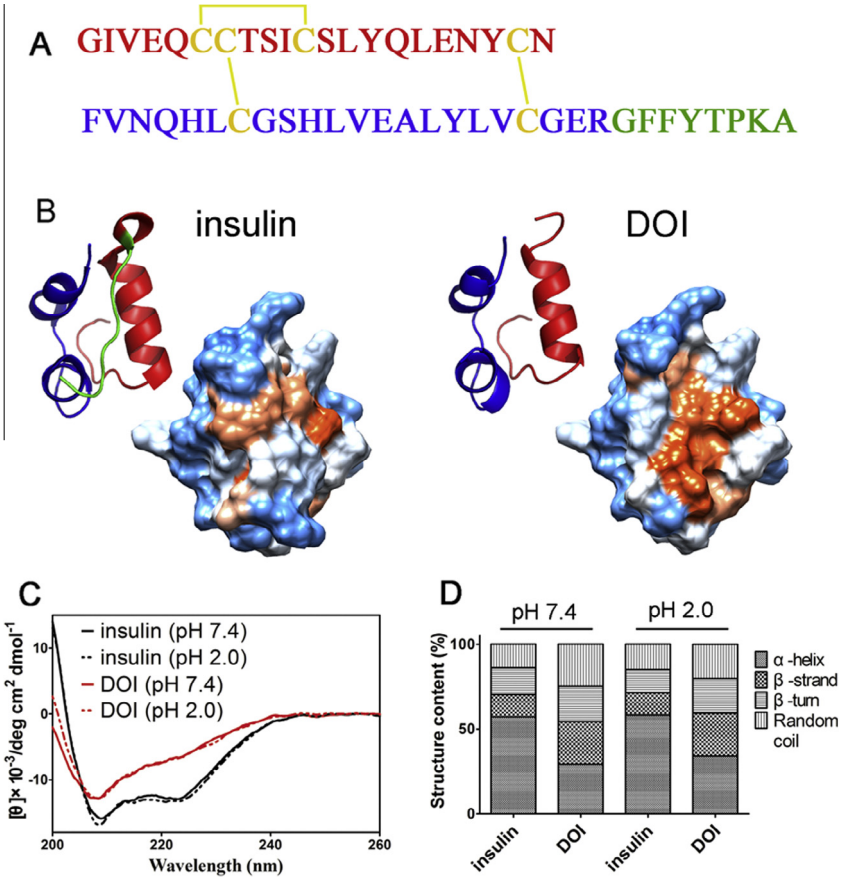

Fig. 1. (A) Primary structure of porcine insulin and DOI. (B) Surface model of porcine insulin and DOI. The hydrophilic residues are shown in blue and the hydrophobic residues are shown in orange (PDB accession number 2EFA). (C) Far-UV circular dichroism spectra of porcine insulin and DOI dissolved in phosphate-buffered saline (PBS, 50 mM phosphate, 100 mM NaCl, pH 7.4) and 0.01 N HCl (0.01 N HCl, 150 mM NaCl, pH 2.0). (D) Deconvolution results of CD spectra. (For interpretation of the references to color in this figure legend, the reader is referred to the web version of this article.)

by comparing amyloidogenicity and fibril structure with insulin. A previous study has indicated that DOI forms amyloid more rapidly than intact insulin under neutral condition [12]. In this study, the amyloidogenecity of DOI was measured under both acidic and neutral conditions, and the secondary structures of fibrils were also investigated. Comparative toxicity of insulin and DOI fibrils were also investigated *via* dye leakage and hemolysis assays.

2. Materials and methods

2.1. Materials

Porcine insulin (PI) was obtained from Wanbang Biopharmaceuticals (Xuzhou, China). Trypsin, Thioflavin-T (ThT), 2-oleoyl-1-palmitoyl-sn-glycerol-3-phospho-rac(1-glycerol) sodium salt (POPG) and 2-oleoyl-1-palmitoyl-sn-glycero-3-phosphocholine (POPC) were purchased from Sigma–Aldrich (St. Louis, USA). Fresh blood was drawn from healthy volunteers using heparin as anticoagulant. All other chemicals were of the highest grade available.

2.2. Preparation of samples

The stock solution of trypsin (5 mg/mL) was prepared in 1 mM HCl and PI was dissolved in 50 mM PBS (pH 7.6) to make a final concentration (1.0 mg/mL) for digestion. Then trypsin was added into PI solution to reach a concentration of 40 μg/mL (molar ratio of PI to trypsin was 25:1). After incubated at 37 °C for 12 h, the solution was filtered through a 0.22 μm Millipore filter, and then injected into a Hitachi 2000 HPLC system (Tokyo, Japan). A Kromasil C8 semi-preparative reverse-phase column (NY, USA) was used for separation. Solvents for the mobile phase were water (A) and acetonitrile (B). The gradient elution was a linear gradient 25–40% B for 20 min. The peaks were detected at 280 nm and the molecular weights of each analyte were confirmed by matrix-assisted laser desorption ionization mass (MALDI-TOF).

2.3. Far-UV circular dichroism (CD) and data analysis

CD spectra were performed on JASCO-810 spectropolarimeter (JASCO, Tokyo, Japan) and the data were recorded at 25 °C under a constant flow of N_2 from 260 to 200 nm with a 1 mm pathlength. Porcine insulin and DOI were dissolved to a final concentration of 30 μM in two solutions: (i) phosphate-buffered saline (PBS, 50 mM phosphate, 100 mM NaCl, pH 7.4), (ii) 0.01 N HCl (0.01 N HCl, 150 mM NaCl, pH 2.0). The spectra were recorded at time intervals indicated, with a scanning speed of 50 nm/min, a response time of 1 s and a bandwidth of 2 nm. Each result was given as the average of three measurements. The data were converted to mean residue ellipticity [θ] and were further analyzed using the software package CDPro as described [15].

2.4. Amyloid formation and Thioflavin-T (ThT) fluorescence assays

Insulin and DOI were dissolved in dimethyl sulfoxide (DMSO) and sonicated for 2 min for homogenization. Proteins were made 60 μM in each of the following conditions as we previously

described [13]: (i) phosphate-buffered saline (PBS, 50 mM phosphate, 100 mM NaCl, pH 7.4), (ii) 0.01 N HCl (0.01 N HCl, 150 mM NaCl, pH 2.0). All sample solutions contained 0.5% DMSO (control study demonstrated that 0.5% DMSO had no effect on fibrillation, data not shown). Samples at pH 2.0 were incubated at 65 °C without agitation. Samples in PBS with 0.01% NaN_3 were incubated at 37 °C and rocked on a table rotary shaker at 20 rpm. Solutions were aliquoted at designated time intervals and thioflavin-T (ThT) based fluorescence assays were used to detect the formation of amyloid. The experiments were performed on a Hitachi FL-2700 fluorometer. The excitation and emission wavelengths were set at 450 and 485 nm, respectively. The solution for quantification contained 50 mM PBS (pH 7.4), 100 mM NaCl and 20 μM thioflavin-T. All experiments were repeated for at least three times. The kinetic curves were calculated as we previously described [13].

2.5. Transmission electronic microscopy (TEM)

TEM was performed as we previously described [3], briefly, 5 μl sample of amyloid fibrils was applied onto a 300-mesh Formvar–carbon coated copper grid (Shanghai, China) and then stained with 1% fresh prepared uranyl formate. After air dried, the sample was observed under an H-8100 transmission electron microscope (Hitachi, Tokyo, Japan) with an accelerating voltage of 150 kV.

2.6. Infrared microscopy

Fibrils formed by insulin and DOI were centrifuged and washed with pure water, and then lyophilized. Infrared spectra of solid samples were recorded using a VERTEX 70 infrared system equipped with a Hyperion TM 2000 IR microscopy (Bruker, Billerica, USA). In brief, the lyophilized samples were placed on a KCl pill and then the absorption measurement was done in the frequency range between 1000 cm^{-1} and 4000 cm^{-1} with a resolution of 4 cm^{-1} and 256 scans.

2.7. Dye leakage assays

POPG and POPC (a molar ratio of 4:1) were dissolved in chloroform to make a concentration of 10 mg/mL. Chloroform was then removed under a stream of N_2, and samples were dried under vacuum to remove residual chloroform. Multilamellar vesicles were made by mixing dry films with 50 mM PBS (100 mM NaCl, pH 7.4) containing 40 mM carboxyfluorescein. PD-10 columns (Sangon, Shanghai, China) were then used to remove nonencapsulated carboxyfluorescein as previously described [16]. Multilamellar vesicles containing carboxyfluorescein were diluted in 50 mM PBS (100 mM NaCl, pH 7.4) for florescence measurements. Amyloid fibrils formed under neutral condition were added to multilamellar vesicles at a final concentration of 20 μM immediately before measurement.

The samples were excited at a wavelength of 493 nm, and the emission was detected at 518 nm. The fluorescence signal was recorded for 30 s, multilamellar vesicles alone were tested as the baseline and the signals of multilamellar vesicles treated with 0.2% (v/v) Triton X-100 (for complete membrane leakage) were used as the positive control. All measurements were repeated for at least three times.

2.8. Hemolysis assay

Hemolysis assay was performed as described [17]. Fresh blood was centrifuged at 1000*g* for 10 min, and erythrocytes were separated from plasma and washed three times with isotonic phosphate buffered saline (pH 7.4). For hemolytic assay, cell suspensions (1% hematocrit) were incubated at 37 °C for 4 h in the presence of 60 μM amyloid fibrils of insulin or DOI. An aliquot of the reaction mixture was removed and centrifuged at 1000*g* for 10 min. Absorbance of the supernatant was determined at 540 nm. The hemolytic rate was calculated in relation to the hemolysis of erythrocytes in 2.5 mM phosphate buffer, which was taken as 100%.

2.9. Dynamic light scattering (DLS)

DLS was performed by using a zeta pals potential analyzer (Brookhaven Instruments Corp., NY, USA). After incubated in neutral conditions for designated time, samples of PI or DOI were transferred into the cuvette in the analyzer, the mean particle size was recorded at a 90° angle for three times.

2.10. Statistical analysis

All results were expressed as the mean ± SD. To evaluate statistical significance, data variance was analyzed with the Kruskal–Wallis test, followed by the Mann–Whitney test. Difference was considered statistically significant at $P < 0.05$.

3. Results

3.1. Preparation of desoctapeptide-(B23–B30) insulin (DOI)

The digestion of porcine insulin was carried out at pH 7.6, under which trypsin has high efficiency to cleave the peptide bond between B22-Arg and B23-Gly. After incubated at 37 °C for 12 h, the mixture was injected into an RP-HPLC system. In addition to insulin, there were two new peaks appearing in the chromatogram (Fig. S1). The MALDI-TOF Mass measurements confirmed the two new peaks as octapeptide-(B23–B30) and DOI, respectively (data not shown).

3.2. Removal of C-terminal of B-chain induces decrease of ordered structure in aqueous sulution

In solution, globular proteins usually show dynamic conformations [18,19]. The secondary structures of insulin and DOI were analyzed by far-UV CD spectroscopy, which measures the average secondary structure that related to amyloidogenicity [13]. In far-UV region, the spectra of DOI were significantly different from those of insulin which showed less ordered structure (Fig. 1C). Deconvolution results (Fig. 1D) showed that insulin had 57.2% and 58.2% α-helical contents at pH 7.4 and pH 2.0, while DOI had 29.2% at pH 7.4 and 34.1% at pH 2.0, respectively, which indicated that DOI markedly exhibited more decreased α-helical contents than the native molecule.

3.3. Exposure of the hydrophobic patch accelerates amyloid formation

To investigate the effect of exposing the hydrophobic patch on amyloidogenicity of insulin, ThT-based fluorescence was performed to monitor the kinetics of amyloid formation. At pH 2.0 and 65 °C, insulin and DOI readily formed amyloids. Compared to insulin (2.41 ± 0.13 h), DOI showed a significantly decreased lag time (0.89 ± 0.06 h, $P < 0.0001$, Fig. 2). At pH 7.4 and 37 °C, the same trend was also observed (Fig. 2B and Table 1). Insulin had a lag time of 1.21 ± 0.06 days, whereas DOI had a much shorter lag time (0.14 ± 0.02 days, $P < 0.0001$, Fig. 2).

Morphologies of insulin and DOI fibrils were observed by TEM. Both of them formed typical long linear fibrils at pH 2.0 and 65 °C after 12 h incubation (Fig. 2C and D), and meshes of fibrils were

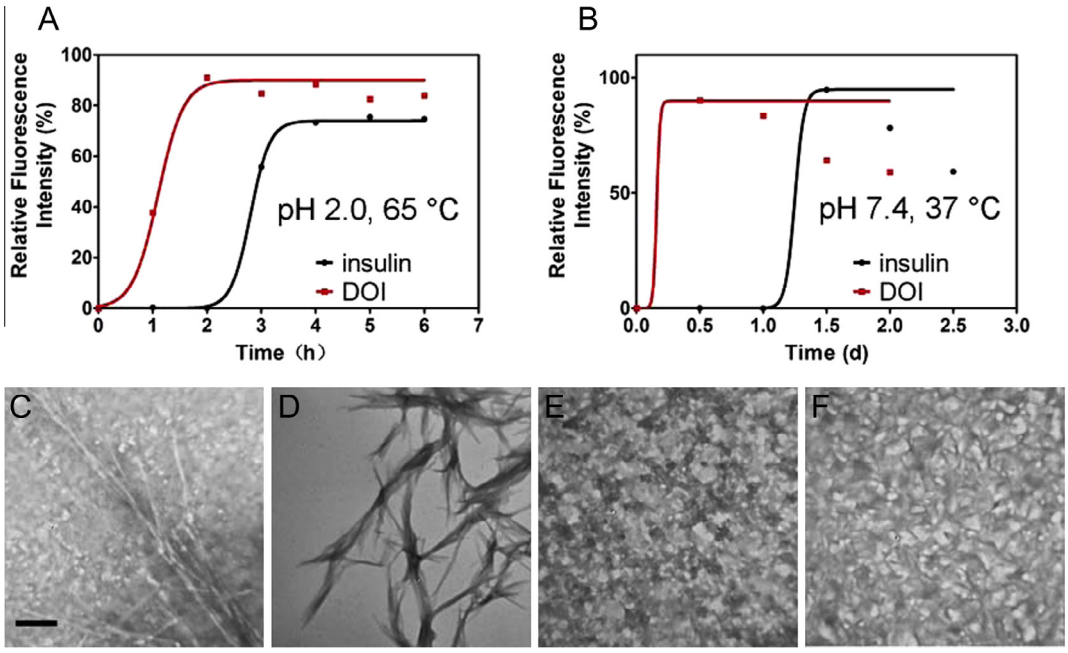

Fig. 2. Amyloidogenicity of insulin and DOI. (A and B) Relative thioflavin-T fluorescence intensity of insulin and DOI incubated at (A) pH 2.0, 65 °C and (B) pH 7.4, 37 °C without agitation. (C–F) TEM morphologies of insulin and DOI fibrils under (C and D) acid and (E and F) neutral conditions. Scale bar equals 200 nm.

Table 1
Lag time of insulin and DOI.[a]

Proteins[b]	pH 2.0		pH 7.4	
	Lag time (h)	Intensity (%)[c]	Lag time (days)	Intensity (%)[c]
Porcine insulin	2.41 ± 0.13	82.9 ± 11.9	1.21 ± 0.06	105.2 ± 5.0
DOI	0.89 ± 0.06	100.0 ± 26.0	0.14 ± 0.02	100.0 ± 14.0

[a] All assays were repeated for at least three times.
[b] The concentration of proteins was 60 μM.
[c] The fluorescence intensity of DOI was set as 100%.

observed for both samples formed under neutral condition (Fig. 2E and F).

3.4. Secondary structure of insulin and DOI fibrils

Infrared microscopy was used to study the secondary structures of insulin and DOI fibrils. The IR spectra of monomer and fibrils of insulin and DOI in amide I region (1600–1700 cm^{-1}) were shown in Fig. 3. All spectra were observed in solid state. There was an evident band at 1659 cm^{-1} indicating α-helix structure in the spectrum of insulin (Fig. 3A) and an intense band at 1630 cm^{-1} indicating β-sheet structure in the spectra of insulin fibrils (Fig. 3C and E) [20]. Compared to insulin, DOI had less α-helix structure in monomeric state (Fig. 3B), which is consistent with the CD results. For fibrils, DOI fibrils were similar to those of insulin formed under acidic condition, whereas insulin fibrils formed under neutral condition showed less β-sheet contents.

3.5. Membrane damage and hemolysis of erythrocytes induced by fibrils of samples

Amyloid fibrils formed by proteins have been reported to cause membrane damage and eventually cell apoptosis [16,21]. Here, we performed dye leakage assays that used artificial micelles containing fluorescence dye to probe the membrane damage capacity of amyloid fibrils formed by insulin and DOI, respectively. It was interesting to find that DOI fibrils caused significantly less

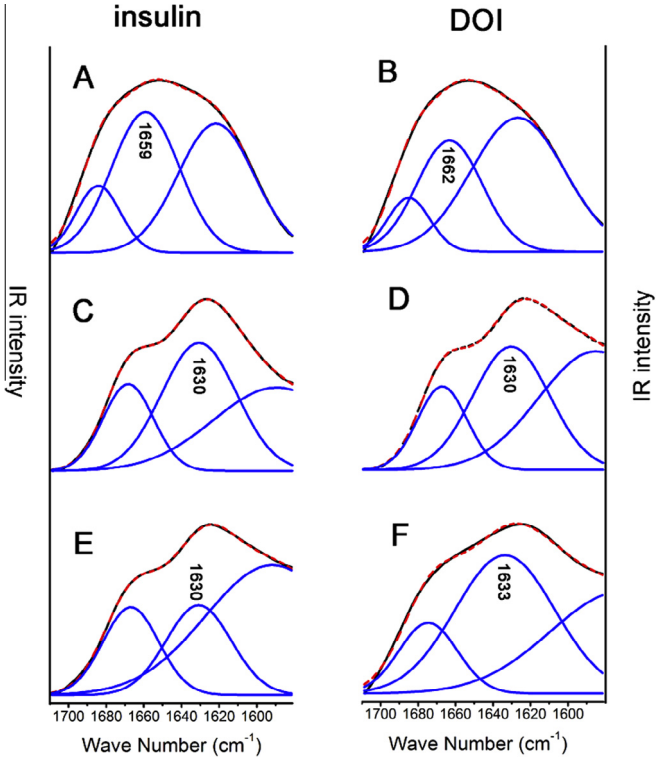

Fig. 3. Expansion of amide I IR region with deconvolution: (A) insulin and (B) DOI monomer, (C) insulin and (D) DOI fibrils formed under acidic condition, (E) insulin and (F) DOI fibrils formed under neutral condition. In each case experimental and fitted spectra are shown in black and red (nearly superimposed as the top trace in each panel). Three component bands that represent total amide I band intensity are in blue. (For interpretation of the references to color in this figure legend, the reader is referred to the web version of this article.)

membrane damage (13.4 ± 0.6%) than insulin fibrils (37.3 ± 5.0%, $P = 0.0012$, Fig. 4A).

Previous studies demonstrated that insulin oligomers and fibrils can cause hemolysis of erythrocytes by disrupting cell membranes

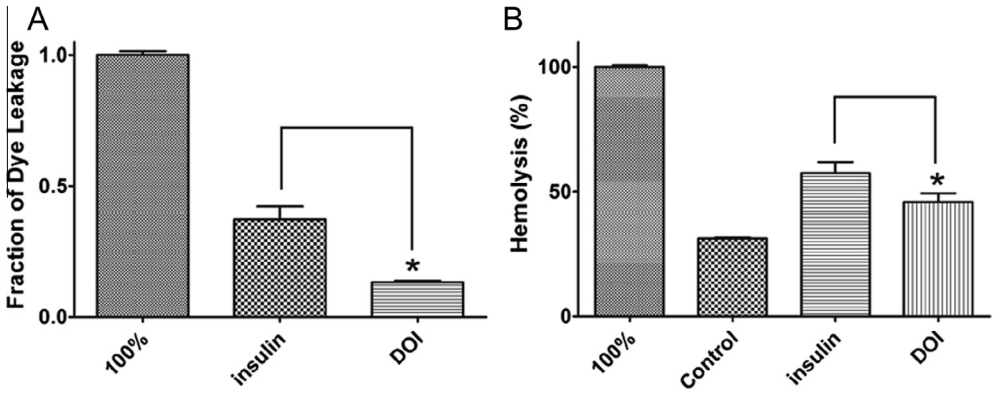

Fig. 4. (A) Fraction of dye leakage of multilamellar vesicles induced by insulin and DOI fibrils. 2% Triton-X treated multilamellar vesicles were used as 100%. (B) Hemolysis of erythrocytes induced by insulin and its analogues after 24 h incubation. Hypotonic solution treated erythrocytes were used as 100% and untreated were used as controls. $^{*}P < 0.0500$.

[22]. In this study, erythrocytes were incubated with insulin and DOI fibrils for 4 h in isotonic environment. The hemolysis of erythrocytes levels for control cells was 31.2 ± 0.4%, while 57.4 ± 4.6% for insulin fibrils and 45.9 ± 3.4% for DOI fibrils, respectively (Fig. 4B). The results showed that DOI fibrils induced significantly less hemolysis of erythrocytes than insulin fibrils ($P = 0.0251$).

4. Discussion

In this study, we used DOI, an insulin analog, to investigate the effect of exposing a hydrophobic patch on amyloidogenicity and fibril structure of insulin. In monomeric state, the removal of B-chain C-terminal induced DOI to expose more hydrophobic surface than insulin (Fig. 1B). As the B-chain C-terminal plays a role on stabilizing the entire molecule by forming intramolecular interconnections [23], its removal also induced the decrease of ordered structure in aqueous solution (Fig. 1C and D). We therefore proposed that the combined actions of exposing hydrophobic residues and the decrease of ordered structure resulted in accelerated amyloid formation (Fig. 2A and B).

In terms of structures of mature fibrils, DOI fibrils were similar to insulin fibrils formed under acidic condition, whereas insulin fibrils formed under neutral condition showed decreased β-sheet contents (Fig. 3). In addition, the DLS results showed that particle size of insulin fibrils (~4340 nm) was smaller than that of DOI fibrils (~5490 nm, Fig. S2), indicated that DOI formed higher-order polymerized amyloid fibrils than insulin under neutral condition, suggesting exposure of the hydrophobic patch in DOI resulted in increased amyloidogenicity, which led to higher order of polymerization under mild physiological condition (pH 7.4 and 37 °C).

Moreover, we further investigated the toxicities of insulin and DOI fibrils by the dye leakage and hemolysis assays. It is generally accepted that the species that are highly toxic to cells are the pre-fibrillar aggregates and the mature fibrils or plaques have been reported as causing much less harm [24]. Therefore, the high-order polymerized fibrils are less toxic than low-order polymerized fibrils [25]. The dye leakage and hemolysis results are consistent with this theory in that DOI fibrils, which are higher-order polymerized than insulin fibrils as the infrared spectra and DLS results suggested (Fig. 3 and Fig. S2), caused less membrane damage and hemolysis of erythrocytes than insulin fibrils (Fig. 4).

Acknowledgments

This work was supported by the Natural Science Foundation of China (Nos. 81172971 and 81222043), and the Program for New Century Excellent Talents in University (NECT11-0170). The authors are grateful to the Analytical and Testing Center of Huazhong University of Science and Technology, and Research Core Facility of College of Life Sciences, Wuhan University for analytical supports.

Appendix A. Supplementary data

Supplementary data associated with this article can be found, in the online version, at http://dx.doi.org/10.1016/j.bbrc.2013.09.032.

References

[1] M. Stefani, C.M. Dobson, Protein aggregation and aggregate toxicity: new insights into protein folding, misfolding diseases and biological evolution, J. Mol. Med. (Berl) 81 (2003) 678–699.
[2] V.N. Uversky, A.L. Fink, Conformational constraints for amyloid fibrillation: the importance of being unfolded, Biochim. Biophys. Acta 1698 (2004) 131–153.
[3] X. Zhang, B. Cheng, H. Gong, C. Li, H. Chen, L. Zheng, K. Huang, Porcine islet amyloid polypeptide fragments are refractory to amyloid formation, FEBS Lett. 585 (2011) 71–77.
[4] Y. Li, H. Gong, Y. Sun, J. Yan, B. Cheng, X. Zhang, J. Huang, M. Yu, Y. Guo, L. Zheng, K. Huang, Dissecting the role of disulfide bonds on the amyloid formation of insulin, Biochem. Biophys. Res. Commun. 423 (2012) 373–378.
[5] B.M. Broome, M.H. Hecht, Nature disfavors sequences of alternating polar and non-polar amino acids: implications for amyloidogenesis, J. Mol. Biol. 296 (2000) 961–968.
[6] W. Kim, M.H. Hecht, Generic hydrophobic residues are sufficient to promote aggregation of the Alzheimer's Abeta42 peptide, Proc. Natl. Acad. Sci. USA 103 (2006) 15824–15829.
[7] C.N. Pace, B.A. Shirley, M. McNutt, K. Gajiwala, Forces contributing to the conformational stability of proteins, FASEB J. 10 (1996) 75–83.
[8] J.C. Rochet, Novel therapeutic strategies for the treatment of protein-misfolding diseases, Expert Rev. Mol. Med. 9 (2007) 1–34.
[9] U. Das, G. Hariprasad, A.S. Ethayathulla, P. Manral, T.K. Das, S. Pasha, A. Mann, M. Ganguli, A.K. Verma, R. Bhat, S.K. Chandrayan, S. Ahmed, S. Sharma, P. Kaur, T.P. Singh, A. Srinivasan, Inhibition of protein aggregation: supramolecular assemblies of arginine hold the key, PLoS One 2 (2007) e1176.
[10] K. Huang, S.J. Chan, Q.X. Hua, Y.C. Chu, R.Y. Wang, B. Klaproth, W. Jia, J. Whittaker, P. De Meyts, S.H. Nakagawa, D.F. Steiner, P.G. Katsoyannis, M.A. Weiss, The A-chain of insulin contacts the insert domain of the insulin receptor. Photo-cross-linking and mutagenesis of a diabetes-related crevice, J. Biol. Chem. 282 (2007) 35337–35349.
[11] K. Huang, B. Xu, S.Q. Hu, Y.C. Chu, Q.X. Hua, Y. Qu, B. Li, S. Wang, R.Y. Wang, S.H. Nakagawa, A.M. Theede, J. Whittaker, P. De Meyts, P.G. Katsoyannis, M.A. Weiss, How insulin binds: the B-chain alpha-helix contacts the L1 beta-helix of the insulin receptor, J. Mol. Biol. 341 (2004) 529–550.
[12] J. Brange, L. Andersen, E.D. Laursen, G. Meyn, E. Rasmussen, Toward understanding insulin fibrillation, J. Pharm. Sci. 86 (1997) 517–525.
[13] K. Huang, J. Dong, N.B. Phillips, P.R. Carey, M.A. Weiss, Proinsulin is refractory to protein fibrillation: topological protection of a precursor protein from cross-beta assembly, J. Biol. Chem. 280 (2005) 42345–42355.
[14] M. Landreh, J. Johansson, A. Rising, J. Presto, H. Jornvall, Control of amyloid assembly by autoregulation, Biochem. J. 447 (2012) 185–192.
[15] N. Sreerama, R.W. Woody, Computation and analysis of protein circular dichroism spectra, Methods Enzymol. 383 (2004) 318–351.
[16] H. Gong, X. Zhang, B. Cheng, Y. Sun, C. Li, T. Li, L. Zheng, K. Huang, Bisphenol A accelerates toxic amyloid formation of human islet amyloid polypeptide: a

possible link between bisphenol A exposure and type 2 diabetes, PLoS One 8 (2013) e54198.
[17] J.B. Wang, Y.M. Wang, C.M. Zeng, Quercetin inhibits amyloid fibrillation of bovine insulin and destabilizes preformed fibrils, Biochem. Biophys. Res. Commun. 415 (2011) 675–679.
[18] H.S. Cho, N. Dashdorj, F. Schotte, T. Graber, R. Henning, P. Anfinrud, Protein structural dynamics in solution unveiled via 100-ps time-resolved X-ray scattering, Proc. Natl. Acad. Sci. USA 107 (2010) 7281–7286.
[19] Y. Akdogan, J. Reichenwallner, D. Hinderberger, Evidence for water-tuned structural differences in proteins: an approach emphasizing variations in local hydrophilicity, PLoS One 7 (2012) e45681.
[20] T. Zako, M. Sakono, N. Hashimoto, M. Ihara, M. Maeda, Bovine insulin filaments induced by reducing disulfide bonds show a different morphology, secondary structure, and cell toxicity from intact insulin amyloid fibrils, Biophys. J. 96 (2009) 3331–3340.
[21] B. Cheng, X. Liu, H. Gong, L. Huang, H. Chen, X. Zhang, C. Li, M. Yang, B. Ma, L. Jiao, L. Zheng, K. Huang, Coffee components inhibit amyloid formation of human islet amyloid polypeptide in vitro: possible link between coffee consumption and diabetes mellitus, J. Agric. Food Chem. 59 (2011) 13147–13155.
[22] B. Huang, J. He, J. Ren, X.Y. Yan, C.M. Zeng, Cellular membrane disruption by amyloid fibrils involved intermolecular disulfide cross-linking, Biochemistry 48 (2009) 5794–5800.
[23] J. Brange, G.G. Dodson, D.J. Edwards, P.H. Holden, J.L. Whittingham, A model of insulin fibrils derived from the X-ray crystal structure of a monomeric insulin (Despentapeptide insulin), Proteins 27 (1997) 507–516.
[24] M. Bucciantini, E. Giannoni, F. Chiti, F. Baroni, L. Formigli, J. Zurdo, N. Taddei, G. Ramponi, C.M. Dobson, M. Stefani, Inherent toxicity of aggregates implies a common mechanism for protein misfolding diseases, Nature 416 (2002) 507–511.
[25] M.F. Mossuto, B. Bolognesi, B. Guixer, A. Dhulesia, F. Agostini, J.R. Kumita, G.G. Tartaglia, M. Dumoulin, C.M. Dobson, X. Salvatella, Disulfide bonds reduce the toxicity of the amyloid fibrils formed by an extracellular protein, Angew. Chem. Int. Ed. Engl. 50 (2011) 7048–7051.